Research Paper
Computational Methods for Differential Equations
http://cmde.tabrizu.ac.ir
Vol. *, No. *, *, pp. 1-21
DOI:10.22034/cmde.2026.67114.3183

Investigation of heat transfer with partial slip on MHD flow of hybrid nanofluid($Cu\!-\!Al_2O_3$/PAO Oil) through a stretching cylinder

Ravi Gupta[1] **and Bharat Kumar**[2,*]
[1]School of Science and Technology, Vardhman Mahaveer Open University, Kota, 324010, India.
[2]Multanmal Bhikhchand Chhajer, Government Girls College, Barmer, 344001, India.

Abstract

The study investigates heat transfer and flow structure of ($Cu - Al_2O_3$/Poly-alpha-olefin oil) hybrid nanofluid over a porous stretching cylinder considering variable viscosity ($\mu_{shnf}(T)$) and thermal conductivity ($k_{shnf}(T)$) with partial slip. We apply similarity transformations to reduce governing PDEs into nonlinear ODEs and solve it using MATLAB's BVP4C solver. The variation of several physical parameters on velocity, temperature, heat transfer rate and skin friction are discussed through graphs and tables. The velocity and temperature profile decreases with increment into partial slip and viscosity parameter. The heat transfer rate increases with increment into partial slip, viscosity and thermal conductivity parameters. The heat transfer enhancement is 9.29% for nanoparticles concentration (Cu : Al_2O_3 - 2% : 1%) and 9.26% for nanoparticles concentration (Cu : Al_2O_3 - 1% : 2%) in hybrid nanofluid, and higher with increase concentration of Cu nanoparticles compared to Al_2O_3 nanoparticles into hybrid nanofluid. The novel part of this study is to investigates heat transfer of MHD hybrid nanofluid ($Cu\!-\!Al_2O_3$/PAO oil) through a stretching cylinder with partial slip using variable viscosity and thermal conductivity.

Keywords. Stretching cylinder, Partial slip, MHD flow, Variable viscosity and thermal conductivity, Porous medium.
2010 Mathematics Subject Classification. 65L05, 34K06, 34K28.

1. Introduction

Hybrid nonofluid defined as mixture of two or more solid nanosize(100-200nm) particles into base fluid, it has interesting field of research in modern time because of their industrial applications. These nanoparticles can be metal, their oxide, carbides, and organic substances. The hybrid nanofluids are widely use in solar energy, heat exchanging system, nuclear cooling system, transformer cooling, electronic cooling and biomedical. The first time, S.U.S. Choi et al [5] introduced the concept of nanofluid, and studied about thermal conductivity of nanofluid. Since, then wide research has been done on nanofluid exploring their properties such as heat transfer, thermal conductivity, diffusivity and viscosity. R. Gupta et al [10, 11] investigated thermal radiation impact of MHD nanofluid considering marangoni convection flow over a stretching surface. S. Saranya et al [28] investigated about unsteady hybrid ferrofluid over a cylinder taking magnetic and cobalt ferrite ferroparticles using shifted Legendre collocation method. The investigation about steady boundary layer flow of hybrid ferrofluid over a spinning vertical cone was studied by S. Saranya et al [29] by iterative power series method. The impact of PST and PHF heating conditions for swirl flow of ternary hybrid nanofluid over a rotating cone was illustrated by Y. Salah et al [25], using shifted Legendre collocation method. M. Nazeer et al [22] demonstrated about thermal analysis of MHD two phase nanofluid over inclined channel using silver and hafnium nanoparticles into transformer oil base fluid.
The Magnetohydrodynamics(MHD) fluid flow defined as flow of nanofluid which is electrically conducting and imposed magnetic field has wide applications in cooling devices and medical industries. It is effective for controlling the heat and mass transfer in hybrid nanofluid. The different shapes of hybrid nanoparticles play a vital role while study

Received: 03 May 2025; Accepted: 19 August 2026.
∗ Corresponding author. Email: bharatkumargoyal2@gmail.com.

on heat transfer with MHD flow was discussed by Kh. Hossinzadeh et al [14] considering (MWCNT-Ag) hybrid nanoparticles into vertical cylinder. R. Ali et al [2] also studied about MHD flow of silica nanofluid over stretching cylinder with various shapes of nanoparticles and Joule heating effect. The influence of thermal radiation for different types of MHD hybrid nanofluid was investigated by P. Agrawal et al [1] in porous stretching surface. The study about MHD williamson nanofluid and thermal radiation through a stretching cylinder was discovered by M. Bilal et al [3], considering variable thermal conductivity. K.U. Rehman et al [24] investigated heat transfer of MHD Jeffrey fluid considering non linear thermal radiation effect in cylindrical surfaces. Many researcher have been done study on MHD flow and heat transfer of different hybrid nanofluid taking different geometry and configuration in porous media. Refs [4, 6, 7, 9, 13, 16–19, 21, 26].

The study about heat transfer of Darcy hybrid nanofluid described by Z. Ullah et al [32] considering thermal radiation effect for stretching tube surface. The influence of variable viscosity on MHD hybrid nanofluid for cylinder surface considering Stefan blowing and partial slip effect was discovered by J. Kandasamy et al [15]. The influence of variable viscosity on heat transfer and flow structure for nanolubricant(TiO_2/PAO) into the microchannel was examined by O.D. Makinde et al [20]. In view of variable viscosity, O.A. Famakinwa et al [8] investigated about the impact of thermal radiation and viscous dissipation on $(Al_2O_3 - CuO)$/water hybrid nanofluid into two parallel plates. S. Saranya et al [30] studied about homogeneous-heterogeneous reactions for ternary hybrid nanofluid over a surface of stationary/moving flat plate using Tiwari and Dass model. The study about nanofluid flow for a unsteady contracting cylinder considering the impact of thermal, heat generation, homogeneous and heterogeneous reaction was investigated by S. Saranya et al [31]. The investigation about three dimensional casson nanofluid flow with double diffusion effect over a stretching sheet considering thermal radiation, chemical reaction, heat generation/absorption, heat and mass transport impact was studied by M. Samiullah et al [27], using cattaneo-christov double diffusion model. The investigation of MHD hybrid nanofluid flow over a unsteady stretching sheet considering variable viscosity and thermal conductivity was studied by R. Gupta et al [12]. The study of williamson fluid flow through a stretching sheet considering inclined magnetic field and thermal radiation was illustrated by P. Priyadharshini et al [23], using numerical & artificial neural network model.

After comprehensive review of literature, we have observed that many studies has been done on hybrid nanofluid considering various geometry and configuration. As we know external heat and internal friction both influence the viscosity and thermal conductivity of hybrid nanofluid, and it depend on temperature. In previous published research many researcher study on hybrid nanofluid considering constant viscosity and thermal conductivity for sheet and cylinder surface. As far as literature review has been done by us, we didn't find any study on how heat transfer and flow structure of $(Cu - Al_2O_3$/PAO oil) hybrid nanofluid influence by variable viscosity & thermal conductivity with partial slip. We found that these are all gaps in previous study which was not be accomplished. The novel part of this work is to investigates heat transfer for MHD hybrid nanofluid $(Cu - Al_2O_3$/PAO oil) through a stretching cylinder with partial slip considering variable viscosity and thermal conductivity. To accomplished our work we formulate fluid equations and solved it using MATLAB's BVP4C solver. The outcomes are discussed through graphs and tables. Also influence of non dimensional parameters such as prandtl number(P_r), magnetic parameter(M), curvature parameter(γ), external heat generation(Q), unsteadiness parameter(S), slip parameter(N), thermal conductivity parameter(ϵ), viscous dissipation(E_k), biot number(B_i), porosity parameter(P), viscosity parameter(R_1) and volume fractions(δ) on velocity and temperature, skin friction factor and nusselt number are investigated.

2. Formulation of Problem

Consider the unsteady stretching cylinder of radius R with two dimensional MHD hybrid nanofluid $(Cu{-}Al_2O_3$/PAO Oil) flow with variable thermal conductivity(k_{shnf}) and viscosity(μ_{shnf}). In this stretching cylinder the surface velocity along z- direction is $U_w{=}\frac{bz}{(1-\alpha t)L}$ [15]. The characteristic length of stretching cylinder is L and cylindrical coordinates (r, θ, z) are considered. The hybrid nanofluid flow is consider in porous medium including partial slip parameter. In this work viscosity and thermal conductivity of hybrid nanofluid are consider as function of temperature. The temperature near the surface for MHD flow is $T_s = T_\infty + T_r\big(\frac{bz^2}{2\nu_f L}\big)(1-\alpha t)^{\frac{-3}{2}}$ [2] and $T_s - T_\infty > 0$ is taken. A Magnetic field $B = \frac{B^*}{\sqrt{(1-\alpha t)}}$ [2] is applied on stretching cylinder on radial direction. The velocity of cylinder

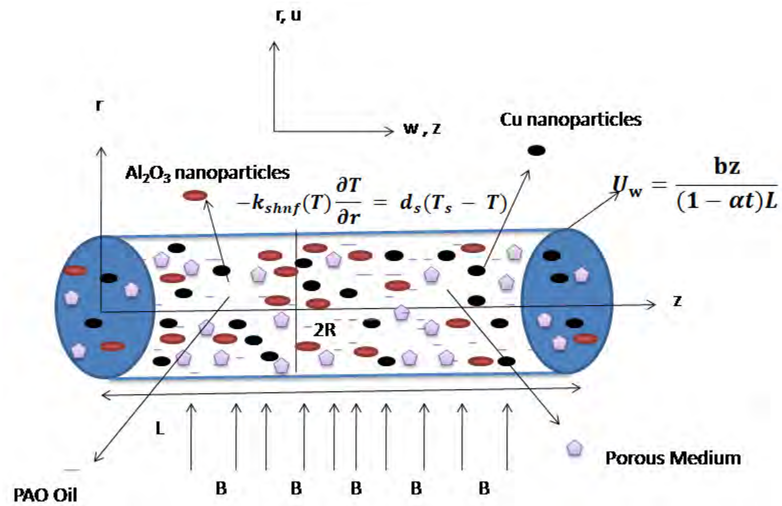

FIGURE 1. Physical representation of flow geometry into stretching cylinder.

is $v(z,r) = (w(z,r), 0, u(z,r))$, where $w(z,r)$, $u(z,r)$ are longitude and transverse components of velocity across the axial and radial direction.

From these considerations the governing PDEs are express as [1, 2]

$$\frac{\partial w}{\partial z} + \frac{u}{r} + \frac{\partial u}{\partial r} = 0, \tag{2.1}$$

$$\frac{\partial w}{\partial t} + w\frac{\partial w}{\partial z} + u\frac{\partial w}{\partial r} = \frac{1}{r\rho_{shnf}}\frac{\partial}{\partial r}\left(r\mu_{shnf}(T)\frac{\partial w}{\partial r}\right) - \frac{\sigma_{shnf}}{\rho_{shnf}}B^2(r,t)w - \frac{\mu_{shnf}(T)}{\rho_{shnf}k^*}w, \tag{2.2}$$

$$\frac{\partial T}{\partial t} + w\frac{\partial T}{\partial z} + u\frac{\partial T}{\partial r} = \frac{1}{r(\rho c_p)_{shnf}}\frac{\partial}{\partial r}\left(rk_{shnf}(T)\frac{\partial T}{\partial r}\right) + \frac{\sigma_{shnf}}{(\rho c_p)_{shnf}}B^2(r,t)w^2 + \frac{\mu_{shnf}(T)}{(\rho c_p)_{shnf}}\left(\frac{\partial w}{\partial r}\right)^2 + \frac{Q^*}{(\rho c_p)_{shnf}}(T - T_\infty), \tag{2.3}$$

The boundary conditions are express as [2, 3]

$$\text{at } r = R; \quad w = U_w + F\frac{\partial w}{\partial r}, \quad u = 0, \quad -k_{shnf}(T)\frac{\partial T}{\partial r} = d_s(T_s - T), \quad r \to \infty; \quad w \to 0, \quad T \to T_\infty, \tag{2.4}$$

By reynold model the variable viscosity is given by [8]

$$\mu_{shnf}(T) = \mu_{shnf}\exp(-R_1\theta(\eta)), \tag{2.5}$$

Using maclaurin series, expanding Eq. (2.5) with omitting higher order terms, we get

$$\mu_{shnf}(T) = \mu_{shnf}\left[1 - R_1\theta(\eta) + \frac{R_1^2\theta^2(\eta)}{2}\right], \tag{2.6}$$

The temperature dependent thermal conductivity is defined as [3]

$$k_{shnf}(T) = k_{shnf}(1 + \epsilon\theta(\eta)), \tag{2.7}$$

where $\epsilon > 0$ and $R_1 > 0$ are thermal conductivity and viscosity parameter, respectively.

Thermophysical characteristic of hybrid nanofluid($Cu - Al_2O_3$/PAO oil) are given by [1, 8]

$$\rho_{shnf} = \rho_{d_1}\delta_1 + \rho_{d_2}\delta_2 + \rho_f(1 - \delta_1 - \delta_2),$$

$$\mu_{shnf} = \frac{\mu_f}{(1-\delta_1)^{2.5}(1-\delta_2)^{2.5}},$$

$$
\begin{aligned}
\sigma_{shnf} &= \sigma_f \left(1 + \frac{3(\frac{\sigma_{d_1}}{\sigma_f} - 1)\delta_1}{(\frac{\sigma_{d_1}}{\sigma_f} + 2) - (\frac{\sigma_{d_1}}{\sigma_f} - 1)\delta_1}\right) \times \left(1 + \frac{3(\frac{\sigma_{d_2}}{\sigma_f} - 1)\delta_2}{(\frac{\sigma_{d_2}}{\sigma_f} + 2) - (\frac{\sigma_{d_2}}{\sigma_f} - 1)\delta_2}\right),\\
(\rho c_p)_{shnf} &= \delta_1(\rho c_p)_1 + \delta_2(\rho c_p)_2 + (1 - \delta_1 - \delta_2)(\rho c_p)_f,\\
\frac{k_{shnf}}{k_f} &= \frac{k_{d_1} + 2k_f + 2(k_{d_1} - k_f)\delta_1}{k_{d_1} + 2k_f - (k_{d_1} - k_f)\delta_1} \times \frac{k_{d_2} + 2k_f + 2(k_{d_2} - k_f)\delta_2}{k_{d_2} + 2k_f - (k_{d_2} - k_f)\delta_2},
\end{aligned}
\tag{2.8}
$$

where δ_1, δ_2 denotes Cu, Al_2O_3 nanoparticles volume fractions and μ_{shnf}, $(\rho c_p)_{shnf}$, σ_{shnf}, ρ_{shnf}, k_{shnf} are dynamics viscosity, heat capacity, electrical conductivity, density, and thermal conductivity of hybrid nanofluid, respectively. The subscripts $shnf$, f, d_1, d_2 represents as hybrid nanofluid, base fluid, first nanoparticle (Cu), and second nanoparticle (Al_2O_3), respectively.

Using suitable transformations and dimensionless variables as [2]

$$
\begin{aligned}
\theta(\eta) &= \frac{T - T_\infty}{T_r\big(\frac{bz^2}{2\nu_f L}\big)(1 - \alpha t)^{-\frac{3}{2}}},\\
\psi &= \frac{zRU_w f(\eta)}{\sqrt{Re}},\\
\eta &= \frac{r^2 - R^2}{2R}\sqrt{\frac{b}{(1 - \alpha t)\nu_f L}},\\
Re &= \frac{zU_w}{\nu_f},
\end{aligned}
\tag{2.9}
$$

where ψ and Re denotes as stream function and reynold number, and η is independent variable.
The longitude(w) and transverse(u) components of velocity are express by [3]

$$
\begin{aligned}
w &= \frac{1}{r}\frac{\partial\psi}{\partial r} = \frac{bz}{(1 - \alpha t)L} f'(\eta),\\
u &= -\frac{1}{r}\frac{\partial\psi}{\partial z} = -\sqrt{\frac{\nu_f b}{(1 - \alpha t)L}}\frac{R}{r} f(\eta),
\end{aligned}
\tag{2.10}
$$

From Eq. (2.9) and (2.10) we reduced Eq. (2.2) and (2.3) into non linear ODEs, which are given by

$$
\begin{aligned}
&(1 + 2\gamma\eta)\frac{D_1}{D_3}\left[\left(1 - R_1\theta + \frac{R_1^2\theta^2}{2}\right)f''' + (-R_1\theta' + R_1^2\theta\theta')f''\right] + 2\gamma\left(1 - R_1\theta + \frac{R_1^2\theta^2}{2}\right)\frac{D_1}{D_3}f''\\
&- M\frac{D_4}{D_3}f' + ff'' - S\left(\frac{\eta}{2}f'' + f'\right) - (f')^2 - P\left(1 - R_1\theta + \frac{R_1^2\theta^2}{2}\right)\frac{D_1}{D_3}f' = 0,
\end{aligned}
\tag{2.11}
$$

$$
\begin{aligned}
&\frac{D_2}{D_5P_r}(1 + 2\gamma\eta)\left[\epsilon(\theta')^2 + (1 + \epsilon\theta)\theta''\right] + \frac{D_1}{D_5}(1 + 2\gamma\eta)\left(1 - R_1\theta + \frac{R_1^2\theta^2}{2}\right)E_k(f'')^2\\
&+ \frac{D_2}{D_5P_r}2\gamma(1 + \epsilon\theta)\theta' - \frac{S}{2}(3\theta + \eta\theta') - 2f'\theta + f\theta' + \frac{D_4}{D_5}M.E_k(f')^2 + \frac{Q}{D_5}\theta = 0,
\end{aligned}
\tag{2.12}
$$

The transformed boundary conditions are

$$
\begin{aligned}
&f(\eta) = 0, \quad f'(\eta) = (1 + Nf''(\eta)), \quad \theta'(\eta) = -\frac{B_i}{A_2}\frac{(1 - \theta(\eta))}{(1 + \epsilon\theta(\eta))}, \quad \text{at} \quad \eta = 0,\\
&f'(\eta) \to 0, \quad \theta(\eta) \to 0, \quad \text{as} \quad \eta \to \infty.
\end{aligned}
\tag{2.13}
$$

The constants D_1, D_2, D_3, D_4 and D_5 are defined as follows

$$
D_1 = \frac{\mu_{shnf}}{\mu_f}, \quad D_2 = \frac{k_{shnf}}{k_f}, \quad D_3 = \frac{\rho_{shnf}}{\rho_f}, \quad D_4 = \frac{\sigma_{shnf}}{\sigma_f}, \quad D_5 = \frac{(\rho c_p)_{shnf}}{(\rho c_p)_f},
\tag{2.14}
$$

The different dimensionless parameters are defined as follows : $\gamma = \sqrt{\frac{(1-\alpha t)\nu_f L}{bR^2}}$ refers to curvature parameter, $S = \frac{\alpha L}{b}$ refers to unsteadiness parameter, $M = \frac{B^{*2}L}{b}\frac{\sigma_f}{\rho_f}$ refers to magnetic parameter, $P = \frac{\mu_f(1-\alpha t)L}{\rho_f k^* b}$ is porosity parameter, $P_r = \frac{(\rho c_p)_f \nu_f}{k_f}$ refers to prandtl number, $E_k = \frac{2\nu_f b}{T_r c_p L\sqrt{(1-\alpha t)}}$ denotes eckert number, $N = F\sqrt{\frac{b}{(1-\alpha t)\nu_f L}}$ is slip parameter, $B_i = -\frac{d_s}{k_f}\sqrt{\frac{(1-\alpha t)\nu_f L}{b}}$ refers to biot number, $Q = \frac{Q^*(1-\alpha t)L}{b(\rho c_p)_f}$ is heat generation parameter.

The Skin friction coefficient(C_f) and Nusselt number(Nu) are represent by [2]

$$C_f = \frac{\tau_w}{\rho_f U_w^2}, \quad Nu = \frac{zq_w}{(T_s - T_\infty)k_f}, \tag{2.15}$$

where coefficient $\tau_w = \mu_{shnf}(T)\big(\frac{\partial w}{\partial r}\big)_{r=R}$, $q_w = -k_{shnf}(T)\big(\frac{\partial T}{\partial r}\big)_{r=R}$ denote as shear stress and heat flux over cylindrical surface and Eq. (2.15) can be transformed into the following form:

$$\begin{aligned} C_f Re^{\frac{1}{2}} &= \frac{\mu_{shnf}}{\mu_f}\left(1 - R_1\theta + \frac{R_1^2\theta^2}{2}\right)f''(0) = \frac{\left(1 - R_1\theta + \frac{R_1^2\theta^2}{2}\right)}{(1-\delta_1)^{2.5}(1-\delta_2)^{2.5}}f''(0),\\ NuRe^{\frac{-1}{2}} &= -\frac{k_{shnf}}{k_f}(1+\epsilon\theta)\theta'(0) = -D_2(1+\epsilon\theta)\theta'(0), \end{aligned} \tag{2.16}$$

In hybrid nanofluid, the heat transfer enhancement is defined as follow [26]

$$H_R = \frac{NuRe^{\frac{-1}{2}}(hybridNanofluid) - NuRe^{\frac{-1}{2}}(Basefluid)}{NuRe^{\frac{-1}{2}}(Basefluid)} \times 100. \tag{2.17}$$

3. Solution Procedure

The transformed non linear ODEs (2.11) and (2.12) together with boundary conditions (2.13) are solved using BVP4C numerical technique in MATLAB. For that we transformed equations into first order ODEs and using following substitutions:

$$\begin{aligned} f &= y_1,\\ f' &= y_2,\\ f'' &= y_3,\\ f''' &= \frac{D_3}{D_1(1+2\gamma\eta)\left(1 - R_1 y_4 + \frac{R_1^2(y_4)^2}{2}\right)}\Bigg[\frac{D_1 P}{D_3}\left(1 - R_1 y_4 + \frac{R_1^2(y_4)^2}{2}\right)y_2 + S\left(\frac{\eta}{2}y_3 + y_2\right) + (y_2)^2\\ &\quad - y_1 y_3 - 2\gamma\left(1 - R_1 y_4 + \frac{R_1^2(y_4)^2}{2}\right)\frac{D_1}{D_3}y_3 + \frac{MD_4}{D_3}y_2 - (1+2\gamma\eta)\frac{D_1}{D_3}\Big(-R_1 y_3 y_5 + R_1^2 y_3 y_4 y_5\Big)\Bigg],\\ \theta &= y_4,\\ \theta' &= y_5,\\ \theta'' &= \frac{D_5 P_r}{D_2(1+\epsilon y_4)(1+2\gamma\eta)}\Bigg[\frac{S}{2}(\eta y_5 + 3y_4) - \frac{\epsilon D_2}{P_r D_5}(1+2\gamma\eta)(y_5)^2 + 2y_4 y_2 - y_5 y_1 - \frac{Qy_4}{D_5}\\ &\quad - \frac{D_4}{D_5}ME_k(y_2)^2 - \frac{D_1}{D_5}E_k(1+2\gamma\eta)\left(1 - R_1 y_4 + \frac{R_1^2(y_4)^2}{2}\right)(y_3)^2 - \frac{2\gamma D_2}{D_5 P_r}(1+\epsilon y_4)y_5\Bigg], \end{aligned}$$

and boundary conditions are defined as

$$y_2(0) = 1 + Ny_3(0), y_1(0) = 0, y_5(0) = -\frac{B_i}{D_2}\frac{(1-y_4(0))}{(1+\epsilon y_4(0)}, y_4(\infty) \to (0), y_2(\infty) \to (0).$$

Table 1. Thermophysical values of hybrid nanoparticle($Cu-Al_2O_3$) and base fluid(PAO Oil) [1, 20].

Physical Characters	Cu	Al_2O_3	PAO oil
Thermal Conductivity $K(\frac{W}{mK})$	401	40	0.143
Specific heat $c_p(\frac{J}{Kg.K})$	385	765	2303
Electrical Conductivity $\sigma(\frac{S}{m})$	5.96×10^7	35×10^6	1.0×10^{-8}
Density $\rho(\frac{Kg}{m^3})$	8933	3970	798

Table 2. Validation with previous finding for Slip parameter(N).

Slip parameter	$f''(0)$		$-\theta'(0)$	
	Ramzan Ali et al [2]	Present	Ramzan Ali et al [2]	Present
0.5	0.801634	0.873638	2.946526	2.824328
1.0	0.565424	0.609644	2.708341	2.690365
1.5	0.439727	0.471471	2.531423	2.558808
2.0	0.360839	0.385535	2.397201	2.449058

4. Results and Discussion

The prime focus is to analyze about heat transfer and flow structure of hybrid nanofluid ($Cu-Al_2O_3$/PAO Oil) into a porous stretching cylinder using variable thermal conductivity and viscosity. We are considering various non dimensional parameters such as volume fraction(δ), curvature parameter(γ), unsteadiness parameter(S), viscosity parameter(R_1), prandtl number(P_r), eckert number(E_k), magnetic parameter(M), heat generation parameter(Q), slip parameter(N), thermal conductivity parameter(ϵ), porosity parameter(P) and biot number(B_i). The outcomes are discussed through graphs and tables, and the influence of Nusselt number and Skin friction are discussed through table. In entire research we are taking $N=0.5$, $\gamma=1$, $M=1$, $S=0.4$, $Q=0.2$, $E_k=0.4$, $R_1=1$, $\epsilon=1$, $B_i=0.5$, $P=1$, $P_r=13$, and $\delta_1=\delta_2=0.02$ and varying all parameters for velocity and temperature.

The thermophysical values of hybrid nanoparticle($Cu-Al_2O_3$) and base fluid(PAO Oil) are reflected by Table 1. Table 2 represents the comparison between current finding to earlier finding considering $f''(0)$ and $-\theta'(0)$ factor for different values of slip parameter(N), when other parameters values are $\gamma=0.3$, $M=0.5$, $S=0.2$, $Q=0$, $E_k=0.5$, $R_1=0$, $\epsilon=0$, $B_i=0$, $P=0$, $P_r=6$, and $\delta_1=\delta_2=0.02$ fixed, the present finding strongly agrees with previous results. The influence of magnetic parameter on velocity, reflected by Figure 2. The magnetic parameter increases from 1 to 4, then velocity profile decreased. Physically, it happened because of Lorentz force which act opposite to fluid flow and decrease the velocity profile. For quantitatively, the term $-Mf'$ into momentum equation represent the Lorentz force and it generate resistance in fluid flow which reduce velocity profile. The relation between unsteadiness parameter(S) with velocity, indicated by Figure 3. It shows that increment in unsteadiness parameter causes decrement into velocity profile, this is because of stretching of the cylinder and it reduces the momentum boundary layer thickness.

The effect of slip parameter(N) on velocity disclosed by Figure 4. It indicates that velocity profile decreases with rising into slip parameter. It happened because of surface irregularity in the presence of slip conditions, and velocity of stretching cylinder is no more equal to velocity of hybrid nanofluid. The effect of curvature parameter(γ) on velocity demonstrated by Figure 5. It indicates that velocity profile decreases near stretching cylinder and increase away from cylinder surface when we increase curvature parameter. The acceleration into curvature parameter decreases the radius of cylinder and reduces number of particles on surface which decrease the resistance of fluid flow and increased velocity away from stretching cylinder. The impact of eckert number(E_k) on velocity disclosed by Figure 6. The outcome shows that velocity decreased with rising into eckert number, because this parameter increase the thermal boundary layer thickness and decrease the kinetic energy of hybrid nanofluid.

The relation between heat generation parameter(Q) and velocity illustrated by Figure 7. The increment in heat generation coefficient decreases the velocity profile, because of decay in momentum boundary layer and impact on velocity is almost negligible. The relation between viscosity parameter(R_1) and velocity investigated by Figure 8. The

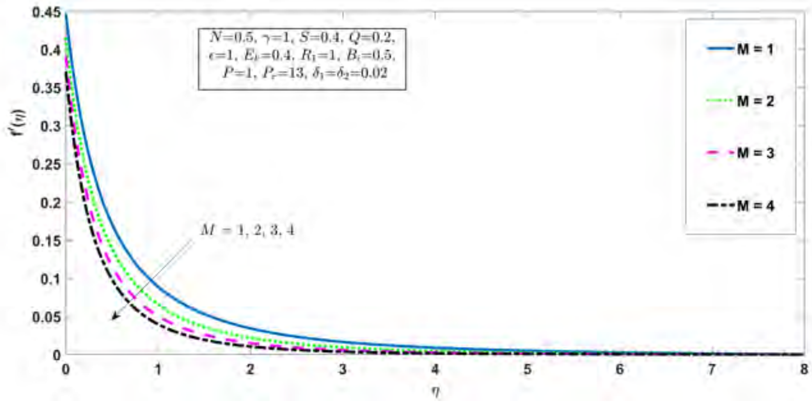

FIGURE 2. Variation in velocity profile for different values of magnetic parameter(M).

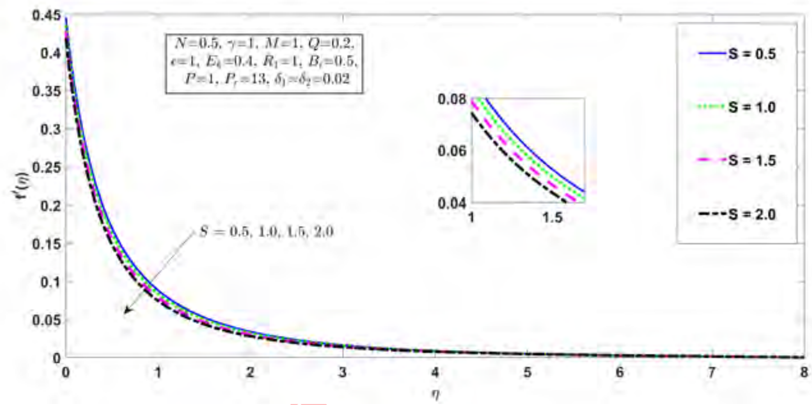

FIGURE 3. Variation in velocity profile for different values of unsteadiness parameter(S).

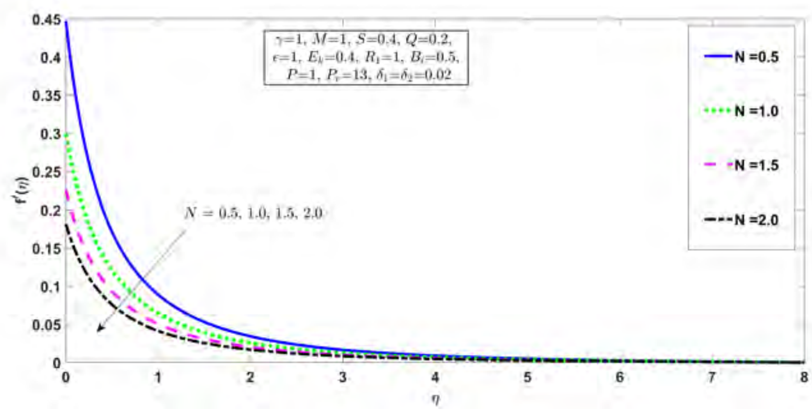

FIGURE 4. Variation in velocity profile for different values of slip parameter(N).

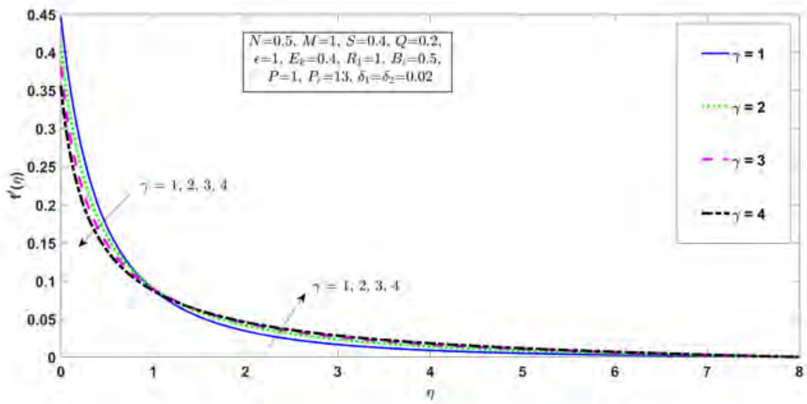

FIGURE 5. Variation in velocity profile for different values of curvature parameter(γ).

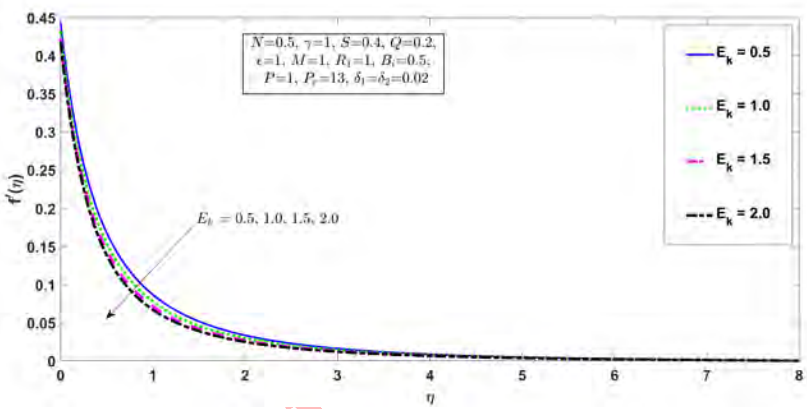

FIGURE 6. Variation in velocity profile for different values of eckert number(E_k).

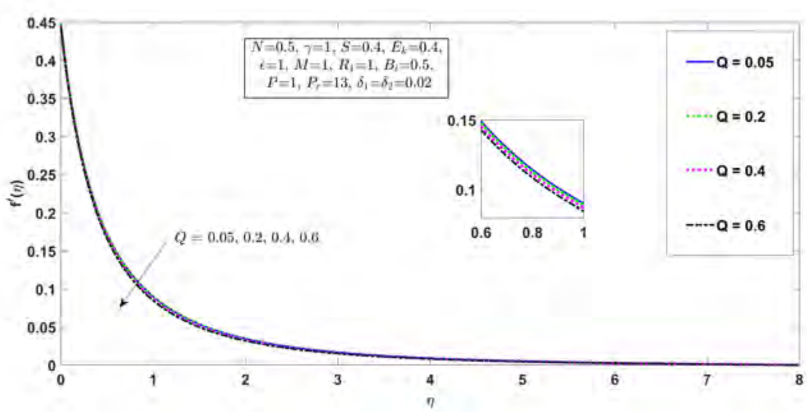

FIGURE 7. Variation in velocity profile for different values of heat generation parameter(Q).

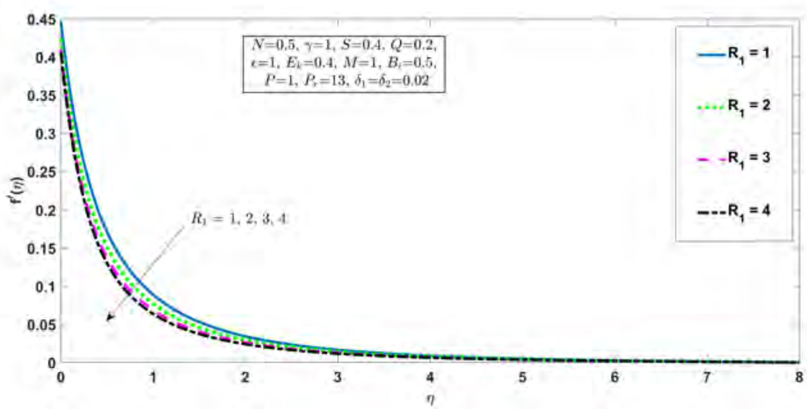

FIGURE 8. Variation in velocity profile for different values of viscosity parameter(R_1).

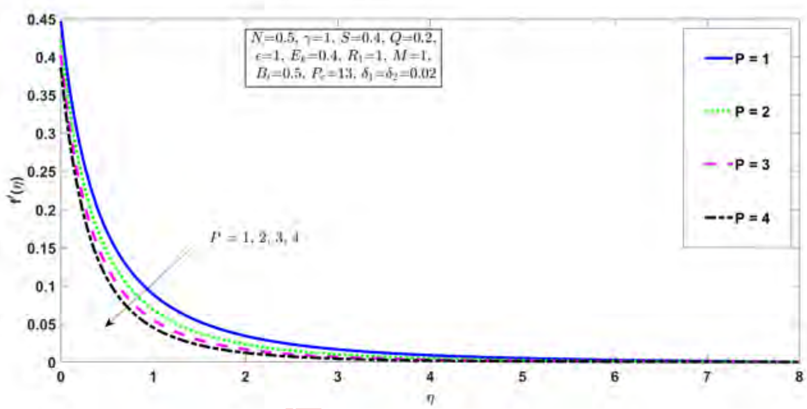

FIGURE 9. Variation in velocity profile for different values of porosity parameter(P).

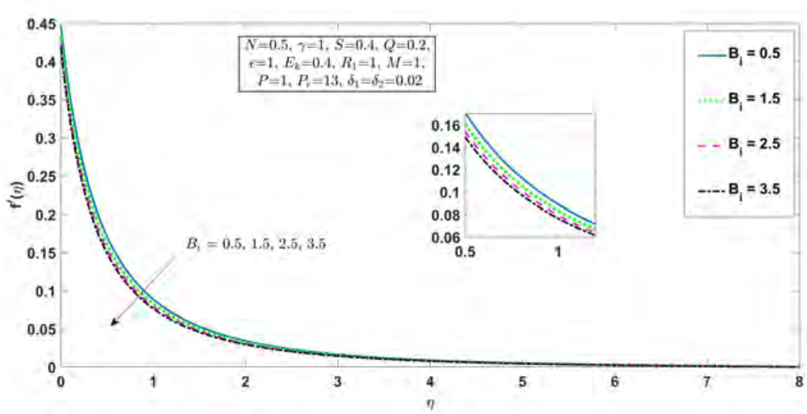

FIGURE 10. Variation in velocity profile for different values of biot number(B_i).

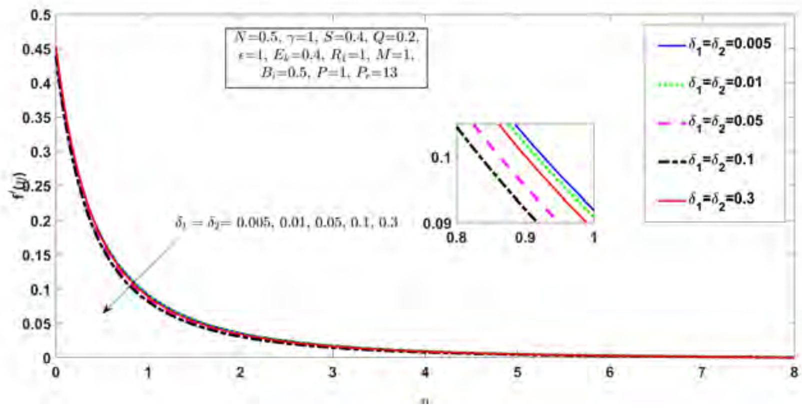

FIGURE 11. Variation in velocity profile for different values of volume fractions δ_1 and δ_2.

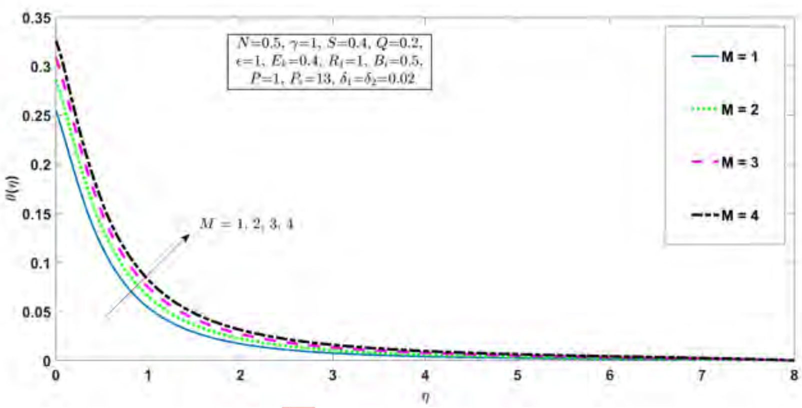

FIGURE 12. Variation in temperature profile for different values of magnetic parameter(M).

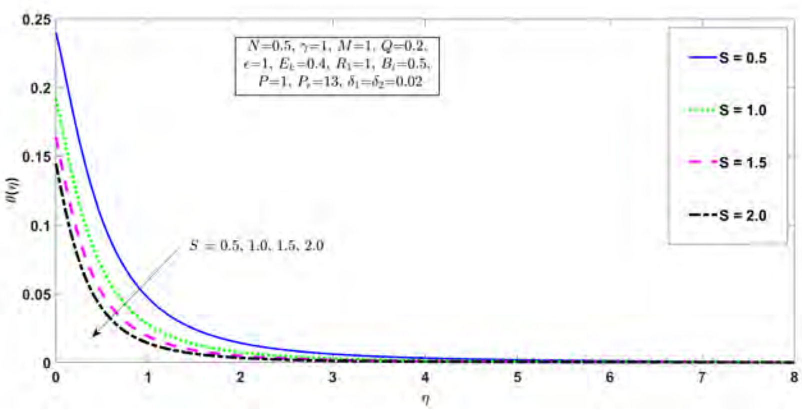

FIGURE 13. Variation in temperature profile for different values of unsteadiness parameter(S).

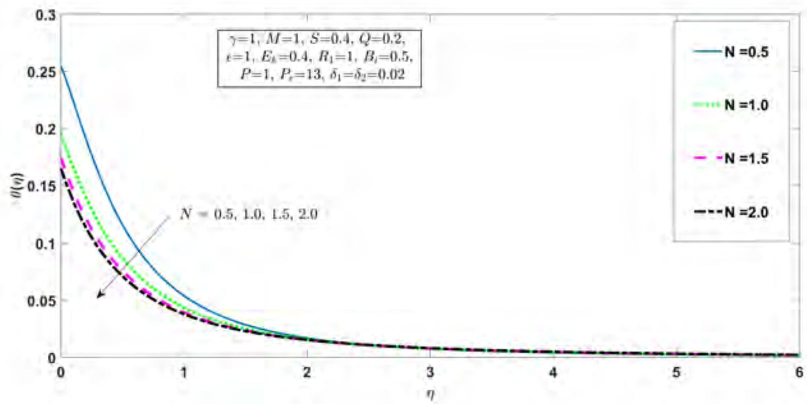

FIGURE 14. Variation in temperature profile for different values of slip parameter(N).

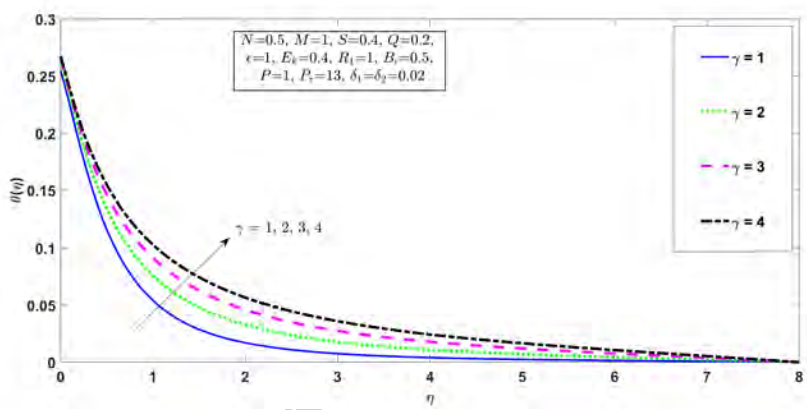

FIGURE 15. Variation in temperature profile for different values of curvature parameter(γ).

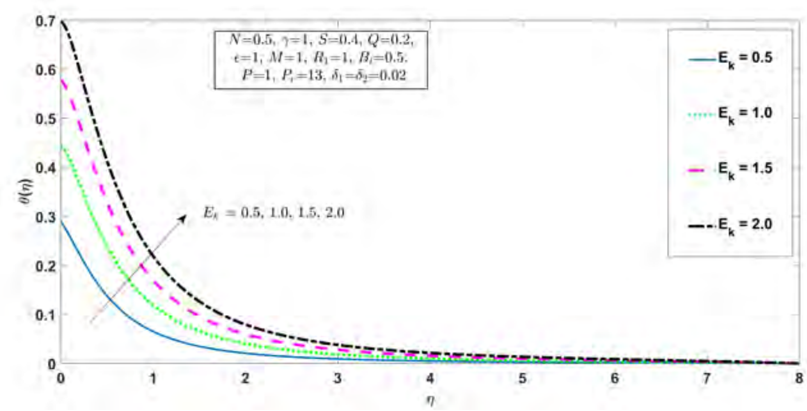

FIGURE 16. Variation in temperature profile for different values of eckert number(E_k).

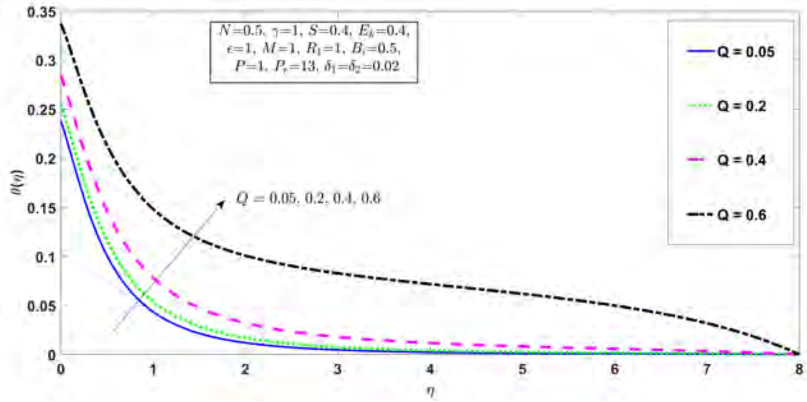

FIGURE 17. Variation in temperature profile for different values of heat generation parameter(Q).

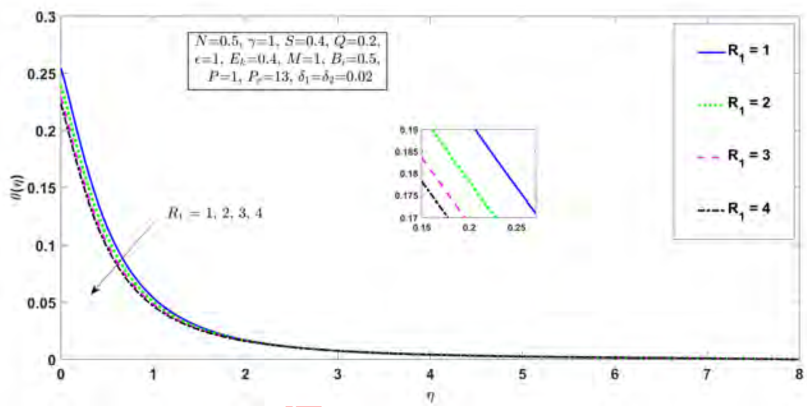

FIGURE 18. Variation in temperature profile for different values of viscosity parameter(R_1).

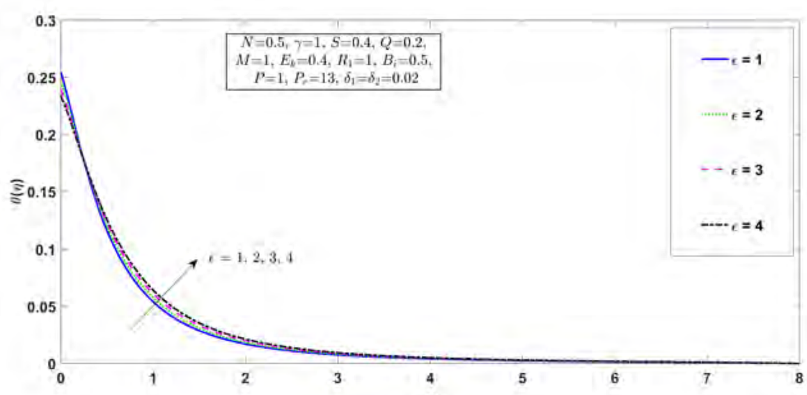

FIGURE 19. Variation in temperature profile for different values of thermal conductivity parameter(ϵ).

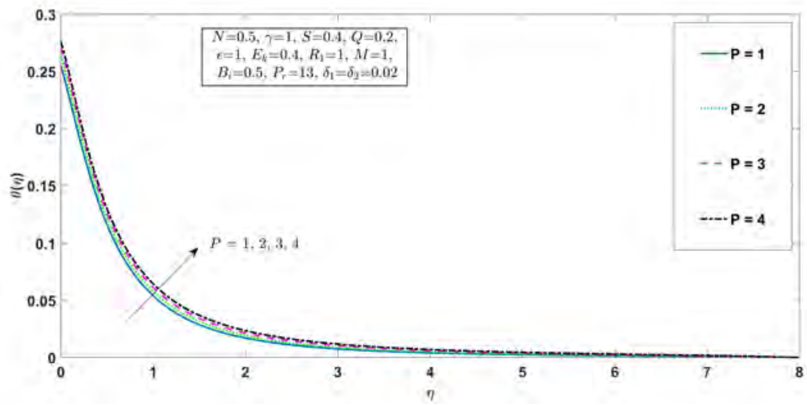

FIGURE 20. Variation in temperature profile for different values of porosity parameter(P).

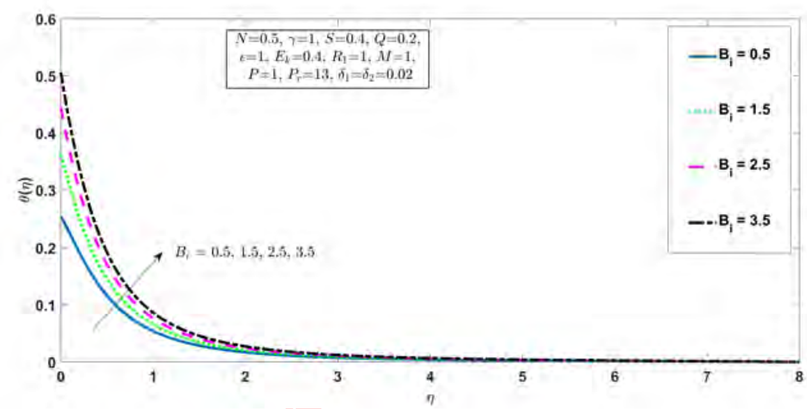

FIGURE 21. Variation in temperature profile for different values of biot number(B_i).

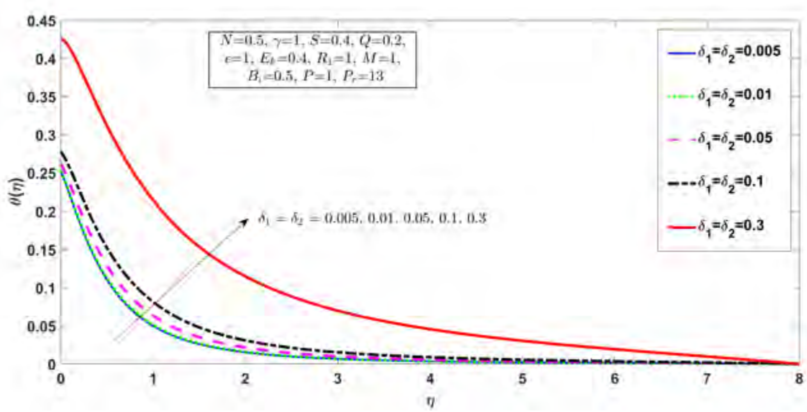

FIGURE 22. Variation in temperature profile for different values of volume fractions δ_1 and δ_2.

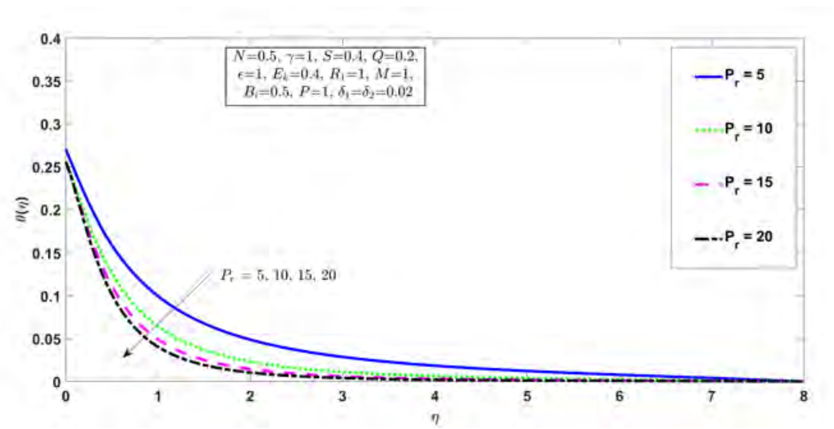

FIGURE 23. Variation in temperature profile for different values of prandtl number(P_r).

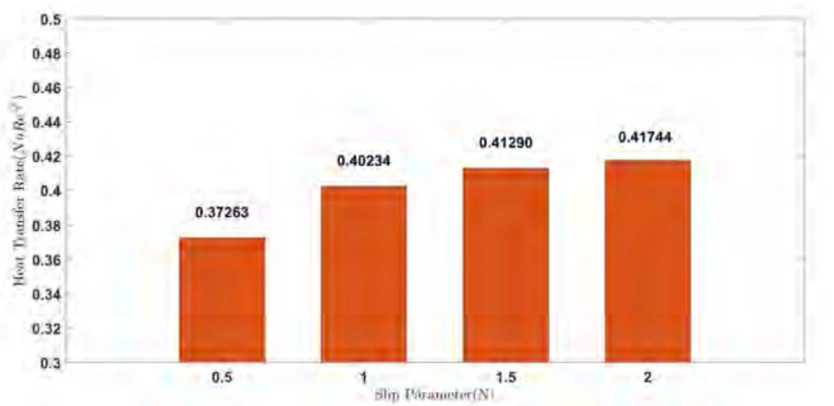

FIGURE 24. Influence of slip parameter on heat transfer rate.

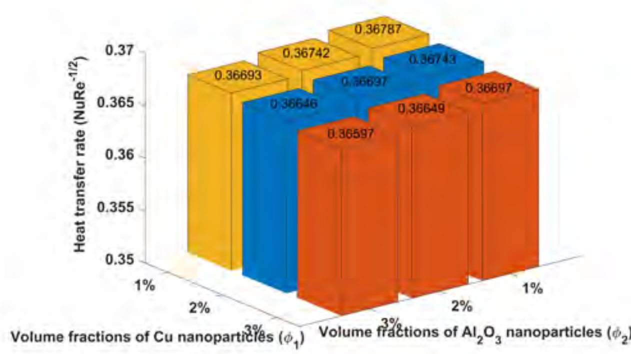

FIGURE 25. Influence of volume fractions on heat transfer rate.

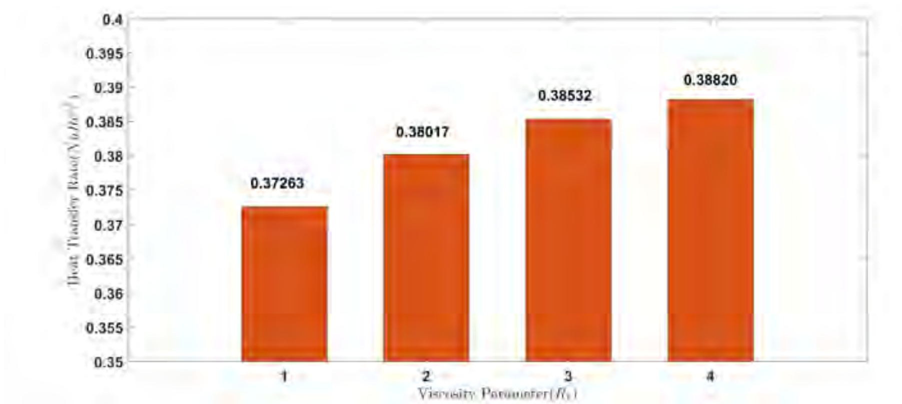

FIGURE 26. Influence of viscosity parameter on heat transfer rate.

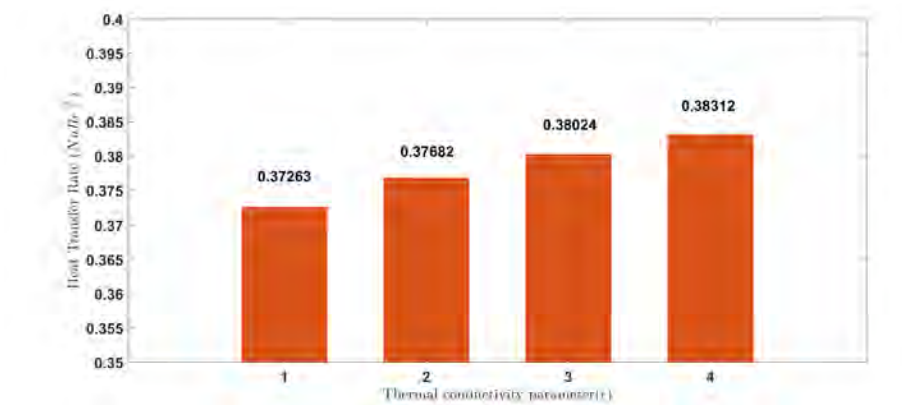

FIGURE 27. Influence of thermal conductivity parameter on heat transfer rate.

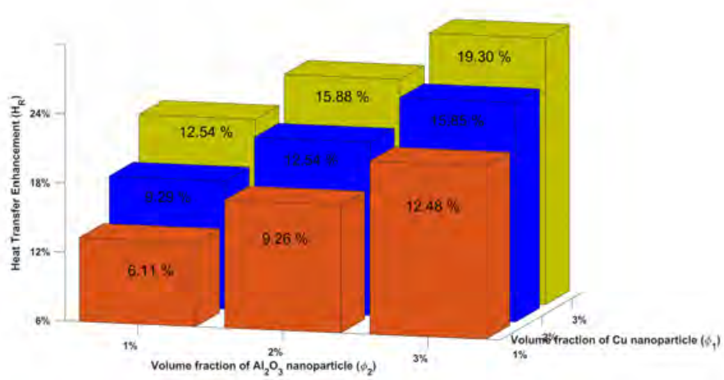

FIGURE 28. Influence of volume fractions on heat transfer enhancement.

TABLE 3. Numerically analysis of Skin friction and Nusselt number.

Parameters													-$C_f Re^{\frac{1}{2}}$	$NuRe^{\frac{-1}{2}}$
M	S	N	P	γ	R_1	Q	E_k	ϵ	B_i	P_r	δ_1	δ_2		
1													0.951644	0.372635
2													0.976622	0.357052
3													0.996079	0.345655
	0.5												0.968004	0.379920
	1.0												1.030653	0.404020
	1.5												1.076447	0.418182
		0.5											0.951644	0.372635
		1.0											0.638604	0.402340
		1.5											0.480160	0.412901
			1										0.951644	0.372635
			2										0.986171	0.368265
			3										1.013164	0.364819
				1									0.951644	0.372635
				2									1.008474	0.369097
				3									1.054887	0.367256
					1								0.951644	0.372635
					2								0.809618	0.380168
					3								0.716363	0.385321
						0.05							0.965033	0.380961
						0.2							0.951644	0.372635
						0.4							0.927953	0.357766
							0.5						0.925750	0.355209
							1.0						0.823008	0.277721
							1.5						0.752220	0.211336
								1					0.951644	0.372635
								2					0.956443	0.376823
								3					0.960441	0.380240
									0.5				0.951644	0.372635
									1.5				0.881709	0.955439
									2.5				0.834459	1.390821
										5			0.935571	0.364873
										10			0.949222	0.371842
										15			0.952440	0.372714
											0.01	0.01	0.902615	0.373629
											0.05	0.05	1.113767	0.369135
											0.1	0.1	1.445959	0.361153

result shows that velocity decreases with acceleration into viscosity parameter, this phenomenon happened because it opposed the fluid flow due to internal friction. The relation between velocity and porosity parameter(P) signifies by Figure 9. The outcome reveals that velocity decreases with rising into porosity parameter, because porosity medium resist the hybrid nanofluid flow in stretching cylinder. The influence of biot number(B_i) on velocity depicted by Figure 10. The outcome shows that velocity drop down with acceleration into biot number, this phenomenon happened due to loss in convective heat. Figure 11 illustrates the impact of solid volume fraction(δ_1, δ_2) on velocity. We noticed that velocity profile decreases with increment into volume fraction, because increase value of volume fraction leads to increase into viscosity of fluid and nanoparticles attract each other for long time and they resist the fluid flow.

The relation between magnetic parameter(M) and temperature display by Figure 12. The temperature profile accelerate while increment in magnetic parameter due to Joule heating and Lorentz force, and the applied magnetic field generate resisting in heat, which act as volumetric heat, and increase the temperature profile. Figure 13 signifies the relation between unsteadiness parameter and temperature profile. The consequence reveals that temperature inversely related to unsteadiness parameter, this phenomenon arise due to loss in heat by stretching cylinder and less heat transmits from stretching cylinder to hybrid nanofluid. The relation between slip parameter(N) and temperature disclosed by Figure 14. The enhancement in slip parameter decay into the temperature, this happened because it rise the heat transfer rate on cylinder surface, and it decrease the thermal boundary layer thickness. The relation between curvature parameter(γ) and temperature display by Figure 15. The consequence shows that temperature enhance with upsurge into curvature parameter. The curvature parameter increase the thermal boundary layer thickness which diminish the heat transfer rate and as a result temperature increased.

The relation between temperature and eckert number(E_k) presented by Figure 16. The result reveals that temperature upsurge with increment in eckert number. The reason behind that increment in eckert number rise the viscous dissipation and kinetic energy which increase the temperature of hybrid nanofluid. The variation in temperature influence by internal heat generation parameter(Q), illustrated by Figure 17. We noticed that temperature profile increases with increment into heat generation parameter, because increase value of Q indicate the temperature storage into the fluid. The relation between viscosity parameter(R_1) and temperature shown by Figure 18. This figure display that temperature profile decreases with increase into viscosity parameter, this phenomenon occurs because of increment in internal friction which slow the fluid motion and nanoparticles attract each other which reduce the temperature profile. The relation between thermal conductivity parameter(ϵ) and temperature display by Figure 19. It is noticed that temperature decreases near stretching cylinder and rise when we move away from cylinder. This phenomenon occurs because heat transfer rate is higher near stretching cylinder and lower away from cylinder.

Figure 20 demonstrates the relationship between porosity parameter(P) and temperature. The outcome shows that temperature profile increase with rising into porosity parameter. It's occurs because in porous medium heat transfer is higher which leads to increase into temperature. The significance impression of Biot number(B_i) on temperature display by Figure 21. The temperature accelerate with increment in biot number, the reason behind that increase value of biot number causes more convection in fluid. Figure 22 illustrates the variation of solid volume fraction(δ_1, δ_2) on temperature. The increment in solid volume fraction increase the temperature profile, this phenomenon occurs because increment into volume fraction upsurge the thermal conductivity and it rise into thermal boundary layer. Figure 23 highlight the relation between prandtl number(P_r) and temperature profile. The increment in prandtl number diminish into the temperature, this happened because prandtl number increase the fluid viscosity and decrease the thermal boundary layer.

Figure 24 display the relation between slip parameter and heat transfer rate. The heat transfer rate enhance with raising into slip parameter, this phenomenon occurs because slip parameter reduce the boundary layer thickness and heat is transmits from cylinder to hybrid nanofluid rapidly. Figure 25 illustrate the impact of solid volume fractions on heat transfer rate. This Figure shows that heat transfer rate decrease with accelerating into the volume fraction of hybrid nanoparticles. Heat transfer rate is higher when concentration of Cu nanoparticle is higher compared to Al_2O_3 nanoparticle into the hybrid nanoparticles. Figure 26 and 27 demonstrate about viscosity parameter and thermal conductivity parameter with heat transfer rate, respectively. The Heat transfer rate increase with rising into viscosity parameter and thermal conductivity parameter, It occurs because increment in viscosity and thermal conductivity enhance into convective heat and thermal transport in hybrid nanofluid. The relation between heat transfer enhancement with volume fraction of hybrid nanoparticles display by Figure 28. The heat transfer enhancement increases with raising into volume fraction of hybrid nanoparticle and no other physical parameters in our study influence the Heat transfer enhancement. The heat transfer enhancement is 9.29% for nanoparticles concentration (Cu : Al_2O_3 - 2% : 1%) and 9.26% for nanoparticles concentration (Cu : Al_2O_3 - 1% : 2%) in hybrid nanofluid, and higher with increase concentration of Cu nanoparticles compared to Al_2O_3 nanoparticles into hybrid nanofluid. Heat transfer enhancement is comparatively higher, if we increase 1% volume fraction of Cu nanoparticle in place of Al_2O_3 nanoparticle in hybrid nanofluid. It shows that high volume fraction of Cu nanoparticles in hybrid nanofluid increase more heat transfer enhancement in hybrid nanofluid.

The numerical observation of Skin friction and Nusselt number highlighted by Table 3. The result reveals that increment in magnetic parameter(M), unsteadiness parameter(S), porosity parameter(P), thermal conductivity parameter(ϵ), prandtl number(P_r), volume fraction of nanoparticles(δ_1, δ_2), and curvature parameter(γ) increases into skin friction, and opposite trend noticed with enhancement into slip parameter(N), viscosity parameter(R_1), heat generation parameter(Q), eckert number(E_k) and biot number(B_i). The outcome shows that heat transfer rate accelerate with increment into S, N, R_1, B_i, P_r, ϵ, and reverse trend noticed for rising into M, P, γ, Q, E_k, δ_1, δ_2.

5. Conclusion

In this numerical study, we investigates heat transfer and flow properties of unsteady hybrid nanofluid($Cu - Al_2O_3$/PAO oil) into a porous stretching cylinder utilizing variable thermal conductivity and viscosity. Using suitable transformation we reduced governing PDEs into ODEs and solved it by BVP4C technique. The outcomes display by graphs and tables. The following key findings are as listed below:

- As the unsteadiness, slip and viscosity parameters increases, the profile of velocity and temperature decreases.
- The velocity profile diminish, and temperature profile increases with raising into volume fraction of nanoparticles, eckert number, biot number, magnetic, heat generation, porosity and thermal conductivity parameters.
- An increment in thermal conductivity parameter, the temperature profile decreases near stretching cylinder, and increased move away from cylinder.
- The heat transfer rate increases with rising into slip, thermal conductivity and viscosity parameters, and reverse trend noticed for rising into magnetic parameter and volume fractions of hybrid nanoparticles.
- The heat transfer enhancement increases with raising into volume fraction of hybrid nanoparticle, and no other physical parameters in our study influence the heat transfer enhancement.
- The heat transfer enhancement is 9.29% for nanoparticles concentration (Cu : Al_2O_3 - 2% : 1%) and 9.26% for nanoparticles concentration (Cu : Al_2O_3 - 1% : 2%) in hybrid nanofluid, and higher with increase concentration of Cu nanoparticles compared to Al_2O_3 nanoparticles into hybrid nanofluid.

Future work

This present work can be further extend for three dimensional MHD flow of different types of fluids such as casson fluid, ternary hybrid nanofluid and non newtonian viscous fluid taking variable viscosity, thermal conductivity and electrical conductivity. Other surface geometry can be taken like cylindrical surface, double rotating disk, vertical plate etc. Also, this study can be done by ANN(Artificial neural network) technique in Machine Learning with different assumptions. We can also work on stability analysis taking same geometry over shrinking cylinder surface.

List of symbols

T_r	Reference temperature(K) ($T_r > 0$ represent heated stretching cylinder and $T_r < 0$ represent cooled stretching cylinder)
F	Velocity slip coefficient(-) ($F = 0$ represent no slip condition and $F > 0$ represent partial slip occurs)
d_s	Surface heat transfer coefficient($W.m^{-2}.K^{-1}$) (It measures how efficiently heat is transferred from the surface to the fluid)
U_w	Surface velocity($m.s^{-1}$)
b	Stretching rate(-) (It measure how fast cylinder stretched along z direction)
T_s	Surface temperature(K)
t	Time(s)
T_∞	Ambient temperature(K)
k^*	Permeability of porous medium(-)
ϵ	Thermal conductivity parameter(-)
ν_f	Kinematic viscosity coefficient($m^2.s^{-1}$)
B^*	Applied magnetic field strength($Kg.s^{-2}.A^{-1}$)
R	Radius of cylinder(m)
$\frac{b}{(1-\alpha t)}$	Stretching rate(-)
Q^*	Coefficient of heat generation(-)
c_p	Specific heat($m^2.s^{-2}.K^{-1}$)
C_f	Skin friction factor(-)
α	Constant(-)

Nu	Nusselt number(-)
S	Unsteadiness parameter(-)
k	Thermal conductivity($W/m.K$)
N	Slip parameter(-)
$f(\eta)$	Dimensionless stream function(-)
μ	Viscosity coefficient($kg.m^{-1}.s^{-1}$)
B_i	Biot number(-)
ρ	Fluid density($kg.m^{-3}$)
P_r	Prandtl number(-)
L	Characteristic length(m)
M	Magnetic parameter(-)
R_1	Viscosity parameter(-)
P	Porosity parameter(-)
σ	Electrical conductivity($S.m^{-1}$)
γ	Curvature parameter(-)

Author contributions

Ravi Gupta : validation, visualization, conceptualization, writing-review & editing, resources, supervision, methodology.

Bharat Kumar : writing-original draft, problem formulation, data curation, methodology, software, investigation, visualization, formal analysis, writing- review & editing.

Conflict of interest

The work has no conflicts of interest.

Data availability

All data which are utilized in study included into this research.

Funding information

Not applicable.

References

[1] P. Agrawal, P. K. Dadheech, R. N. Jat, D. Baleanu, and S. D. Purohit, *Radiative MHD hybrid nanofluids flow over a permeable stretching surface with heat source/sink embedded in porous medium*, Int. J. Numer. Methods Heat Fluid Flow, *31*(8) (2021), 2818-2840.

[2] R. Ali, A. Iqbal, T. Abbass, T. Arshad, and A. Shahzad, *Unsteady flow of silica nanofluid over a stretching cylinder with effects of different shapes of nanoparticles and Joule heating*, Arch. Thermodyn., *45*(3) (2024), 115–126.

[3] M. Bilal, M. Sagheer, and S. Hussain, *Numerical study of magnetohydrodynamics and thermal radiation on Williamson nanofluid flow over a stretching cylinder with variable thermal conductivity*, Alex. Eng. J., *57* (2018), 3281–3289.

[4] S. Chaudhary, A. Singh, D. Kumar, and D. Baleanu, *Numerical analysis for MHD blood-nanofluid flow through a non-linearly stretched sheet interpolated in a permeable medium along heat generation*, Case Stud. Therm. Eng., *52* (2023), 103786.

[5] S. U. S. Choi and J. A. Eastman, *Enhancing thermal conductivity of fluids with nanoparticles*, The Proceedings of the ASME International Mechanical Engineering Congress and Exposition, San Francisco, Calif, USA, *66* (1995), 99–105.

[6] P. K. Dadheech, P. Agrawal, S. D. Purohit, and D. Kumar, *Study of Flow and Heat Transfer of CuO-Ag/$C_2H_6O_2$ Hybrid Nanofluid over a Stretching Surface with Porous Media and MHD Effect*, Sci. Tech. Asia., *26*(4) (2021), 175-182.

[7] P. K. Dadheech, P. Agrawal, A. Sharma, A. Dadheech, Q. M. Al-Mdallal, and S. D. Purohit, *Entropy analysis for radiative inclined MHD slip flow with heat source in porous medium for two different fluids*, Case Stud. Therm. Eng., *28* (2021), 101491.

[8] O. A. Famakinwa, O. K. Koriko, and K. S. Adegbie, *Effects of viscous dissipation and thermal radiation on time dependent incompressible squeezing flow of* $CuO - Al_2O_3$*/water hybrid nanofluid between two parallel plates with variable viscosity*, J. Comput. Math. Data Sci., *5* (2022), 100062.

[9] A. M. Galal, F. M. Alharbi, M. Arshad, M. M. Alam, T. Abdeljawad, and Q. M. Al-Mdallal, *Numerical investigation of heat and mass transfer in three-dimensional MHD nanoliquid flow with inclined magnetization*, Sci. Rep., *14*(1) (2024), 1207.

[10] R. Gupta, M. Gaur, P. K. Dadheech, and P. Agrawal, *Numerical study of marangoni convection flow of GO nanofluid with* H_2O*-EG hybrid base fluid with non linear thermal radiation*, J. Nanofluids, *11*(2) (2022), 245-250.

[11] R. Gupta, M. Gaur, Q. Al-Mdallal, S. D. Purohit, and D. L. Suthar, *Numerical study of the flow of two radiative nanofluids with marangoni convection embedded in porous medium*, J. Nanomater., *580* (2022), 1-7.

[12] R. Gupta and B. Kumar, *Study of MHD flow of hybrid nanofluid (Graphene-*Al_2O_3*/PAO oil) with variable viscosity and thermal conductivity*, Bol. Soc. Paran. Mat., *43* (2025), 1-23.

[13] S. Gupta, C. P. Jain, N. K. Jangid, V. K. Singhal, and P. K. Jain, *Numerical Simulation for MHD Flow of Powell Eyring Nanofluid with Heterogeneous–Homogeneous Reactions, Arrhenius Energy over a Variable Thickness Stretching Surface*, Int. J. Comput. Meth. Eng. Sci. Mech., *25*(3) (2023), 124–136.

[14] Kh. Hosseinzadeh, A. Asadi, A. R. Mogharrebi, M. Ermia Azari, and D. D. Ganji, *Investigation of mixture fluid suspended by hybrid nanoparticles over vertical cylinder by considering shape factor effect*, J. Therm. Anal. Calorim., *143* (2021), 1081–1095.

[15] J. Kandasamy, M. K. Narayanaswamy, and S. Sivanandam, *Effects of Variable Viscosity in Unsteady Magnetohydrodynamics Hybrid Nanofluid Flow over Stretching/Shrinking Cylinder with Partial Slip and Stefan Blowing*, Nanomanufacturing, *3* (2023), 434–445.

[16] B. Kumar and R. Gupta, *Numerical investigation of hybrid nanofluid (*TiO_2*- *Al_2O_3*/water) through Non-linear Partial differential equations*, Inter. J. Math. Ind., (2026), 264002.

[17] B. Kumar and R. Gupta, *Heat Transfer and Thermal Radiation Inspection of MHD Flow of Hybrid Nanofluid with Variable Viscosity and Thermal Conductivity Using Various Shapes*, ICCK J. Appl. Math., *2*(2), (2026), 173–194.

[18] C. Kumar and K. P. Madasu, *Time-dependent rotational motion of a solid sphere in a Jeffrey fluid with velocity slip*, Phys. Fluids, *37*(8), (2025), 083120.

[19] C. Kumar and K. P. Madasu, *Impact of magnetic field and permeability on the unsteady slow rotation of a sphere: slip condition*, Arch. Mech. Eng., *73*(1), (2026), 79-101.

[20] O. D. Makinde and A. E. Makinde, *Thermal analysis of a reactive variable viscosity* TiO_2*-PAO nanolubricant in a microchannel poiseuille flow*, Micromachines, *14* (2023), 1164.

[21] T. Mehta, R. Mehta, and D. Kumar, *Unsteady Magnetohydrodynamics Flow in the Presence of Permeable Medium through an Upstanding Channel with Persistent Suction and Heat Source*, Sci. Tech. Asia., *25*(1) (2020), 106-122.

[22] M. Nazeer, F. Hussain, and T. Anwar, *Thermal analysis in transformer oil-based MHD two-phase flow of Prandtl fluid through inclined channel*, Comput. methods differ. equ., (2025), 1-25.

[23] P. Priyadharshini and V. Karpagam, *Numerical and artificial neural network model for Williamson fluid flow over a stretching sheet under inclined magnetic field and radiation*, Comput. methods differ. equ., 2025, 1-24.

[24] K. U. Rehman, W. Shatanawi, and Q. M. Al-Mdallal, *A comparative remark on heat transfer in thermally stratified MHD Jeffrey fluid flow with thermal radiations subject to cylindrical/plane surfaces*, Case Stud. Therm. Eng., *32* (2022), 101913.

[25] Y. Salah, O. Al Mukbel, Y. Sabsabi, S. Saranya, Q. M. Al-Mdallal, and F. Mukhamedova, *Influence of PST and PHF heating conditions on the swirl flow of* $Al+ Mg+ TiO_2$ *ternary hybrid water-ethylene glycol based nanofluid with a rotating cone*, Int. J. Thermofluids, *19* (2023), 100371.

[26] S. Saleem, M. Qasim, A. Alderremy, and S. Noreen, *Heat transfer enhancement using different shapes of Cu nanoparticles in the flow of water based nanofluid*, Phys. Scr., *95(5)* (2020), 055209.

[27] M. Samiullah, M. Sagheer, and H. Shahzad, *Rotating casson nanofluid flow with generalized heat and mass transport*, Comput. methods differ. equ., (2025), 1-18.
[28] S. Saranya, Q. M. Al-Mdallal, and S. Javed, *Shifted legendre collocation method for the solution of unsteady viscous-ohmic dissipative hybrid ferrofluid flow over a cylinder*, Nanomater., *11*(6) (2021), 1512.
[29] S. Saranya, L. Baranyi, and Q. M. Al-Mdallal, *Free convection flow of hybrid ferrofluid past a heated spinning cone*, Therm. Sci. Eng. Prog., *32* (2022), 101335.
[30] S. Saranya, F. Z. Duraihem, I. L. Animasaun, and Q. M. Al-Mdallal, *Quartic autocatalysis on horizontal surfaces with an asymmetric concentration: water-based ternary-hybrid nanofluid carrying titania, copper, and alumina nanoparticles*, Phys. Scr., *98*(7) (2023), 075214.
[31] S. Saranya, P. Ragupathi, and Q. M. Al-Mdallal, *Thermal and reactive effects in nanofluid flow around a contracting cylinder under magnetic field influence*, Int. J. Thermofluids, *22* (2024), 100710.
[32] Z. Ullah, I. Zari, T. Gul, I. Ali, W. Alghamdi, and F. Ali, *Darcy-Forchheimer hybrid nanofluid flow with quadratic convection over a stretched tube*, Adv. Mech. Eng., *15*(6) (2023), 1-10.